ELSEVIER

Biophysical Chemistry 94 (2001) 165–173

Biophysical Chemistry

www.elsevier.com/locate/bpc

Electrochemistry and spectroscopy study on the interaction of microperoxidase-11 with lipid membrane

Weimin Huang, Zheling Zhang, Xiaojun Han, Jilin Tang, Zhangquan Peng, Shaojun Dong, Erkang Wang*

State Key Laboratory of Electroanalytical Chemistry and National Analytical Research Center of Electrochemistry and Spectroscopy, Changchun Institute of Applied Chemistry, Chinese Academy of Sciences, Changchun, Jilin 130022, PR China

Received 20 July 2001; received in revised form 10 September 2001; accepted 13 September 2001

Abstract

The interaction of microperoxidase-11 (MP11) with cationic lipid vesicles of didodecyldimethylammonium bromide (DDAB) induces an α-helical conformation from random coil conformations in solution and this change then makes heme macrocycle more distorted. DDAB-induced MP11 conformations were investigated by cyclic votammetry (CV), circular dichroism (CD) and UV-vis spectrometry. All results indicate that the binding of MP11 in solution to DDAB vesicles and the ordered structure formation are driven by mostly electrostatic interaction between negatively charged residues in the undecapeptide and positively charged lipid headgroups on the membrane surface. Upon binding to DDAB, its half-peak potential was also changed. The mechanism of the interaction between MP11 and DDAB was also discussed.

Keywords: Microperoxidase-11; Didodecyldimethylammonium bromide; Electrochemistry; Spectroscopy

1. Introduction

As is known, membranes in living organisms are approximately half phospholipids and half protein and many enzymes function in nature bound to membranes. Membrane interfaces have a potent ability to induce secondary structure in a wide range of membrane-active peptides such as hormones, toxins and antimicrobial peptides. The bilayer of phospholipid is an integral structural unit of biomembranes. A variety of bilayer structure, formed by synthetic lipids have been used to mimic membrane properties, and they furnish unique opportunity to investigate the relationship between structure and function. The vesicle system is a self-closed bilayer aggregate and consti-

* Corresponding author. Fax: +86-431-568-9711.
E-mail address: ekwang@ns.ciac.jl.cn (E. Wang).

0301-4622/01/$ - see front matter
PII: S0301-4622(01)00230-7

tutes one of the most explored models of membranes.

The peroxidases are ferric heme enzymes, which catalyze the oxidation of a variety of substrates by hydrogen peroxide. One of the heme model species for the peroxidases can be obtained from enzymatic cleavage of cytochrome *c* [1,2], microperoxidase-11, which still exhibits peroxidase activity [3]. The heme undecapeptide is a good model to study the electrochemical behavior of heme iron in hemoproteins [4]. Its primary structure where numbers refer to positions in the native cytochrome *c* (cyt. *c*) is shown in Fig. 1. The heme group is covalently bond to the undecapeptide via two thioether bonds between two cysteines and the vinyl groups of the heme; his-18 is coordinated to the heme iron on the 'proximal' site, as in the native cytochrome.

MP11 affords the opportunity to mimic the behavior of the parent macromolecule 'bottom-up', and to study the metalloporphyrin when relatively unshielded but still water soluble over an appreciable pH and concentration range.

The redox potentials of cytochromes are determined by several factors such as the type of axial ligands, hydrogen bonding by axial histidines [5] and the effect of the pH of the medium. Especially, the non-planar structure of the heme influences relevant chemical and photophysical properties (e.g. axial ligand affinity, redox potentials, etc.) [6,7].

In this paper we reported that when MP11 binded to DDAB vesicles by electrostatic interaction, its conformation was changed from random coils to α-helix. Conformation difference increased the non-planar distortions in heme of MP11. Furthermore, the midpoint potential was shifted positively. A physical model for the interaction between MP11 and DDAB vesicles was proposed.

2. Experimental

2.1. Reagents

DDAB was obtained from Acros (Belgium). Microperoxidase-11 (MP11) from horse heart (Sigma Chemical Co.) was used without further purification. Hydrogen peroxide (30%) was pur-

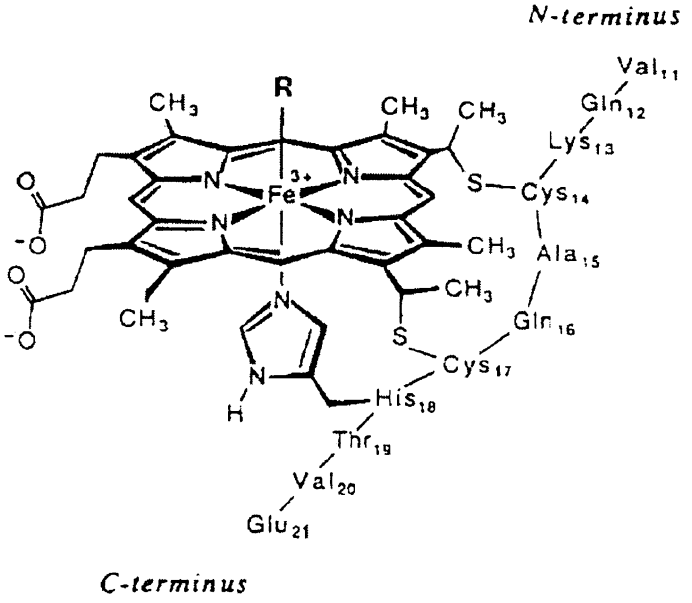

Fig. 1. The structure of microperoxidase-11. The numbering of the amino acid residues refers to the original sequence of cytochrome *c*.

chased from Beijing Chemical Reagent Co. (Beijing, China). The solution of H_2O_2 was prepared daily. The phosphate buffer contained 10 mM phosphate buffer with 0.1 M NaCl. Pure water (18.2 MΩ) was used throughout, obtained by means of a Millipore Q water purification set. All other chemicals were of reagent grade and used as received.

2.2. Sample preparation

Aqueous solution of MP11 was prepared in 10 mM phosphate buffer at pH 6.9. MP11 concentrations were measured spectrophotometrically using a molar absorptivity of 1.76×10^5 M^{-1} cm^{-1} at 395 nm [8]. For the preparation of DDAB vesicles, a dry film of 10 mg of lipid was produced under rotary evaporation from a stock solution in chloroform and then organic solvent was removed by purified nitrogen. The lipid film was hydrated to the desired concentration with 10 mM phosphate buffer, pH 6.9. The resulting multilamellar liposome suspension was sonicated for several hours (in average approx. 2 h) in a bath sonicator, until a clear suspension of small unilamellar vesicles was obtained [9]. The vesicle sizes of a few representative samples were determined by dynamic light scattering measurement on a DynaPro-MS/X dynamic light scattering instrument. The DDAB lipid vesicles had diameters ranging from 40 to 70 nm.

2.3. Preparation of enzyme-modified electrode and cyclic voltammetry

A glassy carbon (GC) electrode (diameter 3 mm) was first polished with sand paper followed by 1.0, 0.3 and 0.05 μm alumina slurry, respectively, then sonicated in deionized water bath for 1 min, three times and then dried at room temperature. MP11 (0.1 mg) and the vesicle of DDAB (10 mg ml^{-1}) were mixed. Of this mixture, 5 μl was spread evenly with a microsyringe onto the surface of the GC electrode. Films were dried gradually overnight with a small bottle covered over the electrode to serve as a closed evaporation chamber, followed by a period of standing in air. The resulting electrode was rinsed with water and stored at 4°C when not in use.

CV was carried out with a CHI 630A electrochemistry workstation (CHI, USA) connected with a Pentium 200 MHz PC. All electrochemical experiments employed a three-electrode cell (5 ml, single electrolyte compartment) with a GC working electrode, a platinum wire auxiliary electrode and an Ag/AgCl (sat. KCl solution) reference electrode. The potential of Ag/AgCl (sat. KCl solution) was taken as 0.198 V vs. SHE. The buffers were purged with purified nitrogen (N_2) for 20 min prior to a series of experiments. A nitrogen environment was kept over solutions in the cell for exclusion of oxygen.

2.4. Absorbance measurements

Absorbance spectra in the Soret (350–450 nm) regions were obtained for samples containing 4.3 μM MP11 in 10 mM phosphate buffer, pH 6.9 in the presence or absence of DDAB vesicles. Typical concentrations of lipid varied from 40 to 400 μM in 10 mM phosphate buffer, pH 6.9. Spectra of the lipid–peptide complexes were measured against a reference-containing lipid vesicle in the same concentration as that in the measuring cell. All spectra were recorded at room temperature on a Cary 500 Scan UV-vis-NIR spectrophotometer (VARIAN, USA).

2.5. Circular dichroism

Circular dichroism spectra were measured in samples of 14 μM MP11 in 10 mM phosphate buffer, pH 6.9, in the presence or absence of lipid vesicles. Spectra was recorded at 25°C on a 62 ADS circular dichroism spectrometer (AVIV Co., USA). Spectra of the far-UV (200–250 nm) and Soret regions were measured using quartz cells of 10 mm path length. Typically, a scanning rate of 50 nm min^{-1}, a time constant of 1 s, and a bandwidth of 1.0 nm were used and 4 scans were averaged per spectrum. Spectra of lipid–protein complexes were subtracted from the background arising from the lipid vesicles alone.

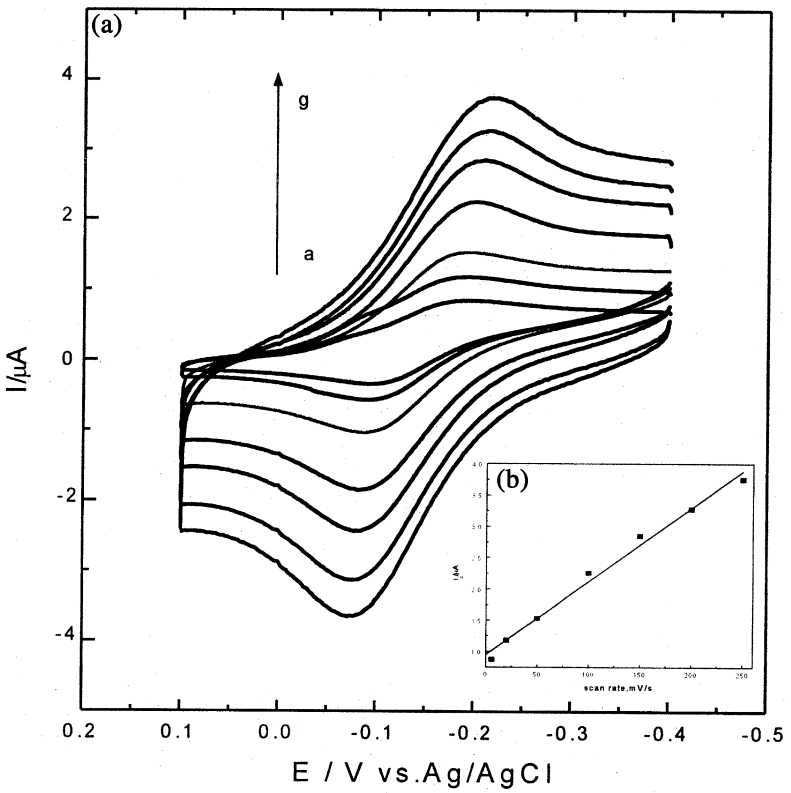

Fig. 2. (a) Cyclic voltammograms of the MP11-DDAB film-modified GC electrode in pH 6.9 phosphate buffer 10 mmol l^{-1}, with 0.1 mol l^{-1} KCl at 25°C. The scan rates are 10, 20, 50, 100, 150, 200, 250 mV s^{-1} from a to g. (b) Influence of scan rate on cathodic peak current for MP11-DDAB film on GC electrode, scan rates: 10; 20; 50; 100; 150; 200; 250 mV s^{-1}.

3. Results

3.1. Cyclic voltammetry

Cyclic voltammograms, as a function of scan rate for MP11-DDAB film on GC electrode in PBS were shown in Fig. 2a. It was also found that neither the bare GC electrode nor the DDAB-modified GC electrode gave any peaks. The electrochemical response for MP11-DDAB film on the GC electrode shows pairs of quasi-reversible ($\Delta E_p = 100$ mV) oxidation/reduction waves. The average half-peak potential for MP11-DDAB on the GC electrode is -143 ± 5 mV (vs. Ag/AgCl/sat. KCl). The half-peak potential is more positive than the value when MP11 were immobilized on the electrode or free in solution [4,10,11]. A positive shift of half-peak potential for MP11 in the presence of a surfactant was also reported in the literature [12]. Furthermore, peak current i_p is proportional to the scan rate v (shown in Fig. 2b), as predicted by the thin layer electrochemistry theory [13].

The catalytic reduction of hydrogen peroxide was performed on the GC electrode with MP11-DDAB film (shown in Fig. 3) as soon as hydrogen peroxide was added into the buffered solution, cyclic voltammograms for the electrode with and without H_2O_2 are shown that MP11 in DDAB film keeps its catalytic activity.

3.2. UV-vis absorption spectra

Heme absorption is a very useful conformational probe for the study of heme proteins as well as positions of the Soret absorption band provid-

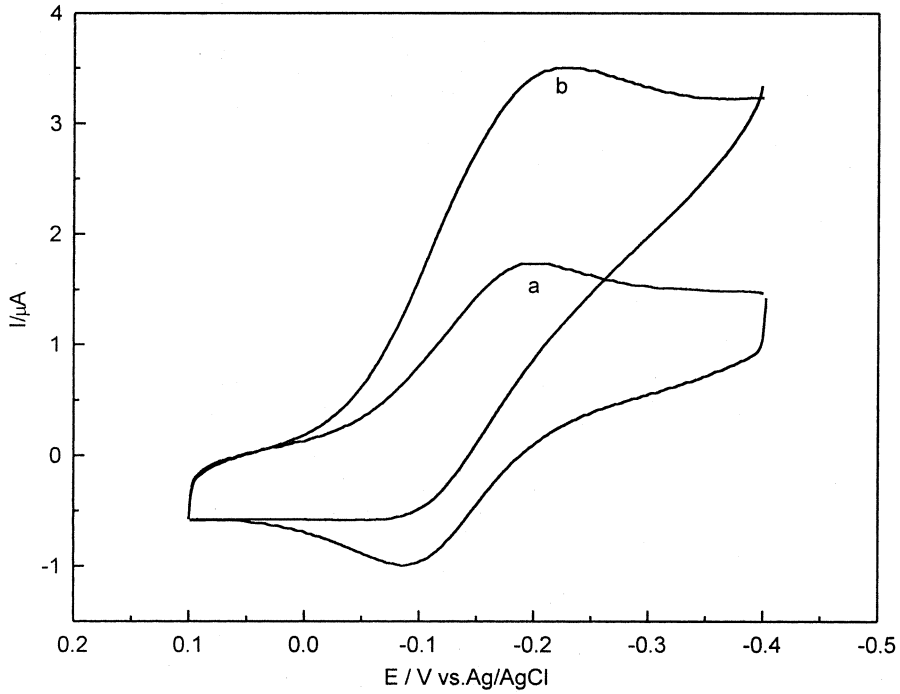

Fig. 3. Cyclic voltammograms of H_2O_2 in pH 6.9 phosphate buffer 10 mmol l^{-1}, with 0.1 mol l^{-1} KCl 25°C, at a GC electrode modified with MP11-DDAB film: (a) no H_2O_2; (b) 1 mmol l^{-1} H_2O_2; scan rate: 50 mV s^{-1}.

ing information about the environment of heme [14] on binding of MP11 to DDAB vesicles. The 400 nm band (shown in Fig. 4, solid line), characteristic of the native random coils of MP11 in solution [8,15], is shifted to 410 nm (shown in Fig. 4, dot line). This red shift is consistent with a more non-planar porphyrin macrocycle [16–18]. This change indicates that a heme status for the binding DDAB vesicles is distinctly different from that in the native protein. The same experiment was done with dimyristoylphosphatidylcholine (DMPC) vesicles, a kind of neutral charge lipid, but no shift was found at 400 nm, only a slight change in peak height (data not shown). This indicates that a heme state for MP11 in the DMPC vesicle is similar to that in the native one. Structural and conformational change may happen when cyt. *c* is binding to oppositely charged lipid vesicles, meanwhile the Soret absorbance in UV-vis of cyt. *c* was also changed. This change was driven by the electrostatic interaction between positive charged residues in the protein and the negatively charged lipid headgroups on the membrane surface [9].

The p*I* of MP11 is 4.7 [8]. When it is in PBS at pH 6.8, MP11 is negatively charged, while DDAB is positively charged. The electrostatic interaction between MP11 and DDAB vesicles may alter the conformation of MP11. In the same time the heme status is also changed by the interaction. The Soret band red shift also indicates a more stable complex between MP11 and DDAB vesicles than random coils MP11 in solution buffer and it may be consistent with a more non-planar porphyrin macrocycle [16].

3.3. CD spectra

CD measurements provided an excellent means of monitoring the interaction between protein and other molecules. Circular dichroism was used to monitor the effects of the interaction with lipid

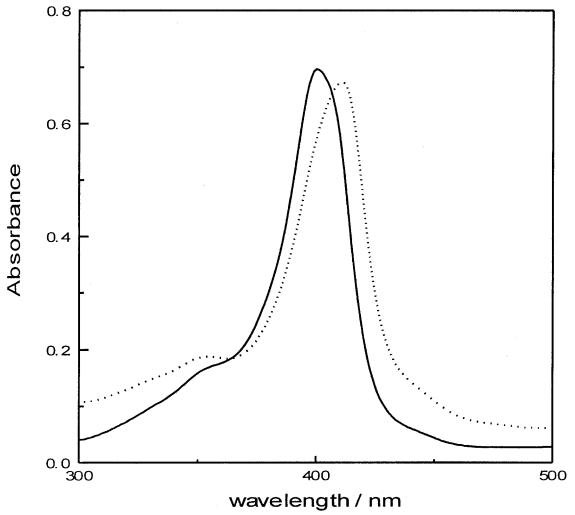

Fig. 4. UV-Vis absorption spectra of MP11 in pH 6.9 phosphate buffer (solid line) and when bound to DDAB vesicles (dotted line), MP11 4.3 μM, DDAB 44 μM. Spectra were obtained at room temperature (25°C), cell path lengths of 1 cm.

vesicles on the structural and conformational properties of MP11. The spectra in the far ultraviolet band provide information about the conformation of the peptide backbone [19]. The far UV-CD spectrum of MP11 in solution shows the presence of only random coil conformations (shown in Fig. 5, solid line) [8,15,20]. Upon binding to DDAB vesicles a dramatic change was observed in the far UV CD band at 209 and 222 nm (shown in Fig. 5, dot line). It shows the typical features characteristic of proteins containing mainly α-helical structure [21,22], in which the 222-nm dichroic band is predominantly associated with α-helical $n-\pi^*$ amide transitions, and the negative minimum at approximately 209 nm are the dichroic bands corresponding to the $\pi-\pi^*$ amide transitions [21,22]. The spectral change around the minimum at 209 nm may be due to the presence of optically active heme transition other than that associated with the amide transition of the polypeptide chain [9]. The fraction of α-helix in MP11 binding to DDAB was 62.5%. The data were calculated from the formula: $\%\ \alpha = 100\ (\Delta\varepsilon_{222} - \Delta\varepsilon_{R})/(\Delta\varepsilon_{H} - \Delta\varepsilon_{R})$ [19,23].

The CD spectra in the Soret region can provide further insight into the integrity of the heme. From the CD spectra of MP11 in PBS (shown in Fig. 6, solid line), appear two proximate bands of opposite sign in the Soret region. When bound upon DDAB vesicles, the two symmetric bands increase dramatically on CD spectrum (shown in Fig. 6, dot line). MP11 does not contain aromatic amino acid residues. Therefore, its considerable optical activity cannot be due to coupling of heme $\pi-\pi^*$ transitions with its aromatic residues [24]. Free unbound heme is not optically active because of the plane of symmetry in its ensemble-average structure. However, when bound to a chiral macromolecule, small but systematic distortions from planarity could generate significant rotational strength in the heme transition [24]. The MP11 retains the thioether linkages and the histidy coordinated to the heme iron. These three points of attachment may suffice to induce a systematic deviation from planarity in the heme in the solution of MP11 [24]. When binding to DDAB vesicles, the extent of non-planar distortion for heme in MP11 increases. This change

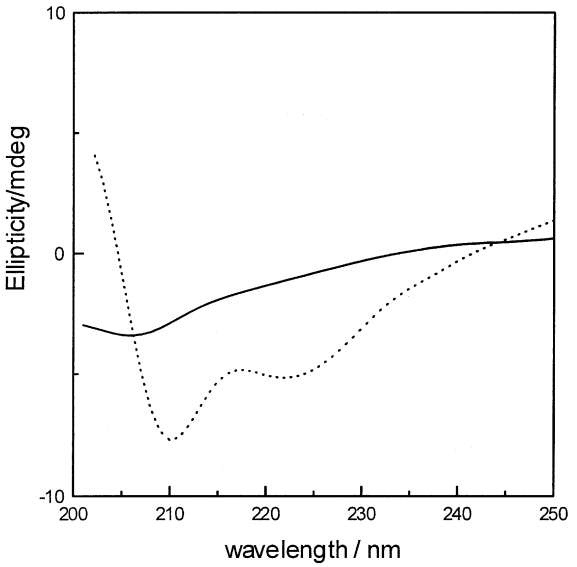

Fig. 5. Far-UV CD spectra of MP11 in pH 6.9 phosphate buffer (solid line) and when bound to DDAB vesicles (dotted line), MP11 14 μM, DDAB 100 μM. Spectra were obtained at room temperature (25°C), cell path lengths of 1 cm; 4 scans were averaged per spectrum.

leads to enhanced CD signal in the Soret region for MP11. The electrostatic interaction and hydrophobic environment provided by DDAB lipid vesicles may induce the native folding of the MP11, because of folding MP11 itself, the peptide backbone exerts the force on the heme macrocycle ruffling and distortion inside MP11.

4. Discussion

Microperoxidase has attracted attention as an interesting model system suitable to gain insight in the structure and electron transfer behavior of the active site of cyt. *c* and more generally of redox metalloproteins. We have shown in this paper that MP11 becomes an ordered and compact structure when binding to DDAB by electrostatic interaction. α-Helix formation in the peptide backbone distorted and ruffled the porphyrin macrocycle. CV results also showed the positive shift of half-peak potential and quasi-reversible characteristics of electrochemistry for MP11 on GC electrodes. It indicates that conformation change from random coils to α-helix for MP11 hinders the electron transfer between MP11 and the electrode. It may prove that the exposure of heme of MP11 diminishes and the distance between the electrode and active site increases. When DMPC was introduced to MP11 solution, no obvious change in UV-vis and CD (data not show). That indicates that only hydrophobic interaction between DMPC and MP11 cannot influence the MP11 conformation. The interaction between DDAB and MP11 may consist of three main steps (shown in Fig. 7).

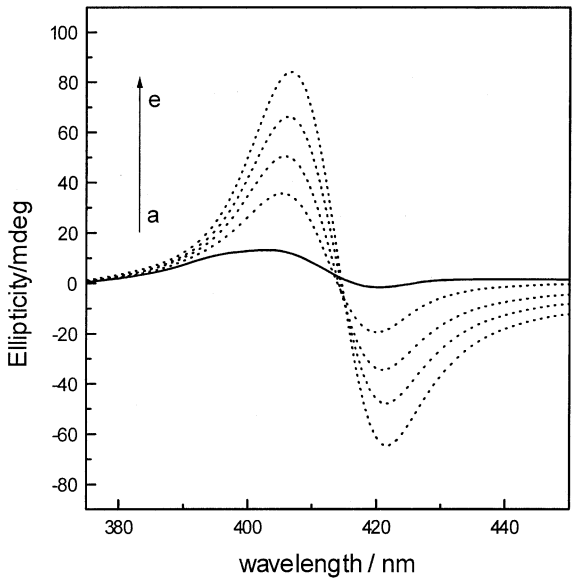

Fig. 6. CD spectra of the Soret region of MP11 in pH 6.9 phosphate buffer (solid line) and when bound to DDAB vesicles (dotted line), MP11 14 μM; DDAB: 50, 100, 200, 400 μM from b to e.

4.1. Unfolded partitioning

The primary cause of favorable partitioning of MP11 from water into a membrane are non-polar interactions, due to expulsion of non-polar compounds (Val11, Ala15, and Val20 of non-polar amino acid) and electrostatic attraction between

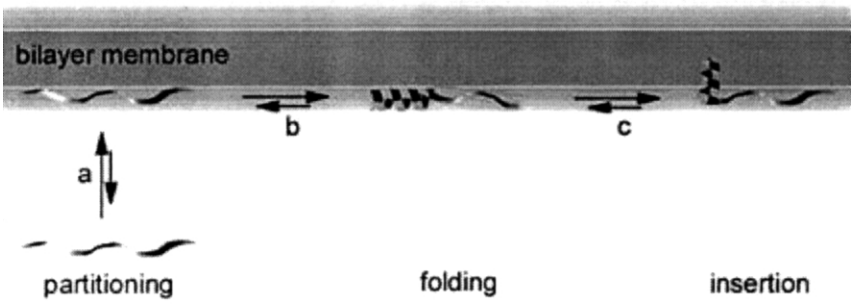

Fig. 7. Scheme of steps about the interaction between DDAB lipid vesicles and MP11 (a) unfolded partitioning; (b) partly folded to α-helix; (c) partial insertion.

basic negatively charged amino acid residues and positively charged DDAB headgroups. From the above UV-vis experimental result, we can conclude that electrostatic interaction plays an important role for the partitioning.

4.2. Partly folded to α-helix

Upon binding to the membrane, the MP11 can change its conformation to α-helix. According to the data obtained by the experiment % $\alpha = 62.5$. We can see that MP11 is partly folded when binding to the DDAB vesicles. In addition, there can be electrostatic effects arising from the differences of the dielectric constants between the water and membrane related to the cost of partitioning H-bonded peptide bonds [25].

4.3. Partial insertion

Actually, for membrane-active peptides, insertion is the last step in folding when binding to membranes [26]. Furthermore, the thermodynamic cost of transferring charged or highly polar uncharged compounds into the oil-like hydrocarbon interior of the bilayer membrane is very high. Increasing ionic strength caused by dissociation, the same result is obtained for cyt. *c* [27]. However, the absorbance spectrum in the Soret band of MP11 is not fully recovered even at a very high ionic strength. Moreover, the N-terminus amino acid of the peptide backbone of MP11 is non-polar (Val11), that gives a possibility for MP11 insertion into the lipid membrane. However, the extent of insertion into lipid vesicles for MP11 is unknown and it needs to be further investigated.

In conclusion, we have observed that binding of MP11 to positively charged lipid membranes induces folding of the random coil structure of MP11 to α-helix. Furthermore, folding in peptide backbone makes heme macrocycle distorted further. In the meanwhile, conformation change gives half-peak potential of MP11 a positive shift. However, MP11 still retains its enzymatic activity. Our findings raise interest with respect to membrane-inactive peptides composed of prosthetic group folding in the membrane environment in particular.

Acknowledgements

This work was supported by the National Natural Science Foundation of China (29835120).

References

[1] J. Aron, D.A. Baldwin, H.M. Marques, J.M. Pratt, P.A. Adams, Hemes and hemoproteins. 1: Preparation and analysis of the heme-containing octapeptide (microperoxidase-8) and identification of the monomeric form in aqueous solution, J. Inorg. Biochem. 27 (1986) 227–243.

[2] J.-S. Wang, H.E. Vanwart, Resonance Raman characterization of the heme *c* group in *N*-acetyl-microperoxidase-8, J. Phys. Chem. 93 (1989) 7925–7931.

[3] O.Q. Munro, H.M. Marques, Heme-peptide models for hemoproteins 1. Solution chemistry of *N*-acetyl-microperoxidase-8, Inorg. Chem. 35 (1996) 3752–3767.

[4] R. Santucci, H. Reinhard, M. Brunori, Direct electrochemistry of the undecapeptide from cytochrome *c* (microperoxidase) at a glassy carbon electrode, J. Am. Chem. Soc. 110 (1988) 8536–8537.

[5] R. Quinn, J.M. Smith, J.N. Burstyn, J.S. Valentine, Influence of hydrogen bonding on the properties of iron porphyrin imidazole complexes. An internally hydrogen bonded imidazole ligand, J. Am. Chem. Soc. 106 (1984) 4136–4144.

[6] K.M. Barkigia, L. Chantranupony, K.M. Smith, J. Fajer, Structural and theoretical models of photosynthetic chromophores. Implications for redox, light absorption properties and vectorial electron flow, J. Am. Chem. Soc. 110 (1988) 7566–7567.

[7] R.G. Alden, M.R. Ondrias, J.A. Shelnutt, Influence of $\pi - \pi$ complex formation, dimerization, and binding to hemoglobin on the planarity of nickel (II) porphyrins, J. Am. Chem. Soc. 112 (1990) 691–697.

[8] M.T. Wilson, R.J. Ranson, P. Masiakowski, E. Czarnecka, M. Brunori, A kinetic study of the pH-dependent properties of the ferric undecapeptide of cytochrome *c* (microperoxidase), Eur. J. Biochem. 77 (1977) 193–199.

[9] T.J.T. Pinheiro, G.A. Elöve, A. Watts, H. Roder, Structural and kinetic description of cytochrome *c* unfolding induced by the interaction with lipid vesicles, Biochemistry 36 (1997) 13122–13132.

[10] L. Jiang, A. Glidle, C.J. McNeil, J.M. Cooper, Characterization of electron transfer reactions of microperoxidase assembled at short-chain thiolmonolayers on gold, Biosensor Bioelectron. 12 (1997) 1143–1155.

[11] T. Ruzgas, A. Gaigalas, L. Gorton, Diffusionless electron transfer of microperoxidase-11 on gold electrode, J. Electroanal. Chem. 469 (1999) 123–131.

[12] D.K. Das, O.K. Medhi, Effect of surfactant and pH on the redox potential of microperoxidase 11 in aqueous micellar solutions, J. Chem. Soc. Dalton Trans. 10 (1998) 1693–1698.

[13] R.W. Murray, Electroanalytical Chemistry, Marcel Dekker, New York, 1984.

[14] G. Irace, E. Bismuto, F. Savy, G. Colonna, Unfolding pathway of myoglobin: molecular properties of intermediate forms, Arch. Biochem. Biophys. 244 (1986) 459–469.
[15] A.M. Jehanli, D.A. Stotter, M.T. Wilson, Magnetic studies on the ferri-haem undecapeptide of cytochrome *c*, Eur. J. Biochem. 71 (1976) 613–616.
[16] J.A. Shelnutt, C.J. Medforth, M.D. Berber, K.M. Barkigia, K.M. Smith, Relationships between structural parameters and Raman frequencies for some planar and nonplanar nickel (II) porphyrins, J. Am. Chem. Soc. 113 (1991) 4077–4087.
[17] L.D. Sparks, C.J. Medforth, M.-S. Park et al., Metal dependence of the nonplanar distortion of octaalkyltertraphenylporphyrins, J. Am. Chem. Soc. 115 (1993) 581–592.
[18] C.J. Medforth, M.O. Senge, K.M. Smith, L.D. Sparks, J.A. Shelnutt, Nonplanar distortion models for highly substituted porphyrins, J. Am. Chem. Soc. 114 (1992) 9859–9869.
[19] J.M. Scholtz, Q. Hong, E.J. York, J.M. Stewart, R.L. Baldwin, Parameters of helix-coil transition theory for alanine-based peptides of varying chain lengths in water, Biopolymers 31 (1991) 1463–1470.
[20] R. Santucci, A. Picciau, G. Antonini, L. Campanella, A complex of microperoxidase with a synthetic peptide: structural and functional characterization, Biochim. Biophys. Acta 1250 (1995) 183–188.
[21] N. Greenfield, G.D. Fasman, Computed circular dichroism spectra for the evaluation of protein conformation, Biochemistry 8 (1969) 4108–4116.
[22] N.J. Greenfield, Methods to estimate the conformation of proteins and polypeptides from circular dichroism, Biochemistry 20 (1981) 33–37.
[23] B. Gopal, K.G. Papavinasasundaram, G. Dodson, M.J. Colston, S.A. Major, A.N. Lane, Spectroscopic and thermodynamic characterization of the transcription antiermination factor NusE and its interaction with NusB from *Mycobacterium tuberculosis*, Biochemistry 40 (2001) 920–928.
[24] G. Blauer, N. Sreerama, R.W. Woody, Optical activity of hemoproteins in the Soret region. Circular dichroism of the heme undecapeptide of cytochrome *c* in aqueous solution, Biochemistry 32 (1993) 6674–6679.
[25] M. Dathe, T. Wieprecht, Structural features of helical antimicrobial peptide: their potential to modulate activity on model membranes and biological cells, Biochim. Biophys. Acta 1462 (1999) 71–87.
[26] N. Ben-Tal, A. Ben-Shaul, A. Nicholls, B. Honig, Free-energy determinants of alpha-helix insertion into lipid bilayers, Biophys. J. 70 (1996) 1803–1812.
[27] M. Rytomaa, P.K. Kinnunen, Evidence for two distinct acidic phospholipid-binding sites in cytochrome *c*, J. Biol. Chem. 269 (1994) 1770–1774.